Heliyon 10 (2024) e21909

Contents lists available at ScienceDirect

Heliyon

journal homepage: www.cell.com/heliyon

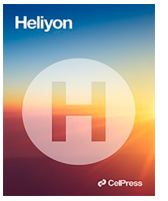

# CPXM1 correlates to poor prognosis and immune cell infiltration in gastric cancer

Qiou Gu [a,1], Lei Mi [b,1], Chuilin Lai [a,1], Xiao Guan [a], Na Lu [a], Tian Zhan [a], Guoguang Wang [a], Chen Lu [a], Lei Xu [a], Xiang Gao [a], Jianping Zhang [a,*]

[a] *Department of General Surgery, The Second Affiliated Hospital of Nanjing Medical University, 121 Jiangjiayuan Road, Nanjing, Jiangsu, 210009, PR China*

[b] *Department of Oncology, Yancheng First Hospital, Affilital Hospital of Nanjing University Medical School, The First People's Hospital of Yancheng, 66 Renmin South Road, Yancheng, Jiangsu, 210009, PR China*

A R T I C L E I N F O

*Keywords:*
Gastric cancer
Carboxypeptidase X (M14 family) member 1
TME
Immune cell infiltration
Drug sensitivity

A B S T R A C T

*Background:* Gastric cancer (GC) is the fourth most common cause of cancer-related death and the fifth most frequent malignant cancer, especially advanced GC. Carboxypeptidase X member 1 (CPXM1) is an epigenetic factor involved in many physiological processes, including osteoclast differentiation and adipogenesis. Several studies have shown the association of CPXM1 with multiple tumors; however, the mechanism of CPXM1 involvement in the progression of GC is yet to be characterized.

*Method:* CPXM1 expression data were obtained from the Tumor Immune Estimation Resource. The Cancer Genome Atlas and the Gene Expression Omnibus databases were used to obtain patient-matched clinicopathological information, and the Kaplan–Meier plot database was utilized for the prognosis analysis of GC patients. The Catalog of Somatic Mutations in Cancer and cBioportal databases were adopted to study CPXM1 mutations in tumors. Next, we utilized the Gene Ontology, Kyoto Encyclopedia of Genes and Genomes, and Gene Set Enrichment Analysis for mechanism research. Furthermore, we performed tumor microenvironment and immune infiltration analysis based on CPXM1. Finally, we predicted sensitivity to several targeted drugs in GC patients based on CPXM1.

CPXM1 is upregulated in GC and is correlated with poor prognosis, gender, and tumor stage in GC patients. Gene enrichment analysis suggested that CPXM1 may regulate the occurrence and progression of GC via the PI3K–AKT and TGF-β pathway. Moreover, CPXM1 expression results in an increase in the proportion of immune and stromal cells. Additionally, the proportion of plasma cells was inversely related to the expression of CPXM1, whereas macrophage M2 expression was proportionate to CPXM1 expression. Finally, six small-molecule drugs that showed notable variations in $IC_{50}$ between two groups were screened.

*Conclusion:* These results suggested that CPXM1 regulates the progression of GC and may represent a novel target for the detection and treatment of GC.

* Corresponding author.
*E-mail addresses:* gqo1993@njmu.edu.cn (Q. Gu), 781896384@qq.com (L. Mi), 1477764980@qq.com (C. Lai), 1477764980@qq.com (X. Guan), ln248457306@qq.com (N. Lu), 302790672@qq.com (T. Zhan), ggwang@njmu.edu.cn (G. Wang), 294646516@qq.com (C. Lu), lxu_njmu_edu@163.com (L. Xu), 2314005924@qq.com (X. Gao).

[1] Qiou Gu, Lei Mi and Chuilin Lai contributed equally to this work.

https://doi.org/10.1016/j.heliyon.2023.e21909
Received 12 December 2022; Received in revised form 14 September 2023; Accepted 31 October 2023
Available online 11 November 2023

## 1. Introduction

Globally, gastric cancer (GC) continues to be one of the most common cancer-related causes of death and the most frequent malignant cancers [1]. It is reported that GC has the third-highest morbidity and ranks fifth among tumor-related mortality [2]. Nearly 90 % of GC cases globally are caused by *Helicobacter pylori* infection. Being overweight, smoking, and a high intake of salt and processed meats. Epstein–Barr virus infection and autoimmune gastritis are additional possible risk factors for GC [3].

Endoscopic resection is the main therapy for patients with early-stage GC. Surgery is used to treat advanced GC, and this procedure should include a D2 lymphadenectomy (removing all lymph nodes within the peri-gastric mesentery and along the celiac arterial branches). Patients with stages 1B GC or higher have a better chance of survival when receiving perioperative or adjuvant chemotherapy. Advanced GC is treated with a platinum and fluoropyrimidine doublet as the first line of chemotherapy; however, the median survival time is less than 1 year [4]. There are numerous difficulties faced in the treatment of GC. The main objective is to achieve early detection and therapy through the implementation of endoscopic screening programs in high-risk areas, as well as the development of reliable diagnostic markers [5]. In general, it is critical to discover novel markers that aid in early detection and therapy [6].

Carboxypeptidases (CPs) play a crucial role in each aspect of human physiology [7]. For example, carboxypeptidase A3 (CPA3) is a special carboxypeptidase located in mast cells and participates in innate immunity, angiogenesis, and remodeling of the extracellular matrix. Thus, CPA3 can be used to help judge the prognosis and improve the effectiveness of targeted therapy [8]. One previous study showed that carboxypeptidase E (CPE) can alter glutamylation of microtubules and the redistribution of $p150^{Glued}$, indicating that CPE may play a big part in the regulation of cortical neuron migration [9]. In another study, the NF-α1/CPE complex was shown to activate the β-inhibin/ERK/CREB/BCL2 axis via 5-HTR1E to provide neuroprotection [10].

Carboxypeptidase X member 1 (CPXM1) belongs to the CP family. A report suggested that CPXM1 is secreted as a collagen-binding glycoprotein and binds to other proteins through a discoidin domain that contains 160 amino acids [11]. It has also been confirmed that CPXM1 can regulate adipogenesis and act downstream of FGF-1/BAMBI, and may promote the expansion of proliferative adipose tissue by influencing extracellular matrix remodeling [12]. Several studies have reported that CPXM1 serves as a biomarker of ovarian cancer [13], breast cancer [14], neck squamous cell carcinoma [15], myelodysplastic syndrome [16], and papillary thyroid [17]. In GC patients with a poor prognosis, primary gastric linitis plastica (GLP) is a unique phenotype of GC. Recently, researchers performed whole exome sequencing and whole transcriptome sequencing on ten tumor–normal tissue pairs; all were GLPs. Six genes, including CPXM1, were found to have significant high levels of mutation in GLP [18]. However, it remains unknown how CPXM1 contributes to GC.

In this study, we examined how CPXM1 contributes to the occurrence and progression of GC.

## 2. Materials and methods

### 2.1. Data sources of tumor and adjacent-tumor tissues of CPXM1

First, data regarding CPXM1 expression in tumor tissue and adjacent-tumor tissue from different kinds of tumors were downloaded from the Tumor Immune Estimation Resource (TIMER) (http://timer.comp-genomics.org) database. We obtained expression and clinicopathological information, including 343 GC tissues and 30 tumor-adjacent tissues, from The Cancer Genome Atlas (TCGA) (https://portal.gdc.cancer.gov) database. In addition, one microarray dataset GSE27342 from the Gene Expression Omnibus (GEO) database (https://www.ncbi.nlm.nih.gov/geo) was also acquired. Survival curves of CPXM1 were obtained from the Kaplan–Meier plot website (https://kmplot.com/analysis/index).

### 2.2. Somatic mutations and alteration of CPXM1 in pan-cancers and GC

All the data containing different kinds of mutations were adopted from the Catalog of Somatic Mutations in Cancer (COSMIC) (https://cancer.sanger.ac.uk/cosmic). Then, we collected and analyzed copy number change data in the cBioPortal database (https://www.cbioportal.org/). Thus, our study used these two databases for CPXM1 mutations in different kinds of tumors, especially in GC.

### 2.3. Clinicopathological correlation analysis of CPXM1 in GC

To evaluate the relationship between CPXM1 and clinicopathological information, the clinicopathological data of patients from TCGA were observed. The "limma" and "ggpubr" packages in R software were adopted for data analysis, and $p < 0.05$ was considered statistically significant.

### 2.4. Identification of differentially expressed genes (DEGs)

We first identified the genes related to CPXM1 expression and defined them as related genes. Based on the mean expression of CPXM1, samples were divided into two groups, the high and low expression group, and the gene profiles between the two groups were compared. DEGs were defined with $p < 0.05$, and logFC $\geq 1$ or $\leq -1$. The detailed genes are shown in a heat map. The "limma," "ggplot2," "ggExtra," and "ggpubr" packages in R software were adopted for data analysis of the related genes. The "limma," "circlize," and "corrplot" packages in R software were adopted to generate the cyclic graphs. Finally, the "limma" and "pheatmap" packages in R

software were adopted to generate the heat map. Statistical significance was set as $p < 0.05$.

### 2.5. Functional enrichment analysis of DEGs

The "or.Hs.eg.db" package was adopted to switch the gene IDs, while enrichment analysis was done using the "clusterProfiler" and "enrichplot" packages. The threshold conditions included were as follows: $p < 0.05$ and $q < 0.2$. Finally, the "limma," "circlize," "RColorBrewer," "dplyr," "ggplot2," and "ComplexHeatmap" packages in R software were adopted for presentation of the functional enrichment results.

### 2.6. Tumor microenvironment (TME) and immune cell infiltration

The "estimate" package in R was used to calculate the TME score, which includes the stromal score and the immune score, and the sum of these two is the ESTIMATE score. We compared the differences between CPXM1 high expression and low expression groups, and the "CIBERSORT" package in R was used to reveal the association between gene expression and immune cell abundance. Finally, the "limma," "reshape2," and "ggpubr" packages in R were used for the violin plot of the TME, and the "reshape2," "vioplot," "ggExtra," "corrplot," and "ggpubr" packages in R were used for images of immune cell infiltration. Statistical significance was set as $p < 0.05$.

### 2.7. Drug sensitivity analysis

The "pRRophetic" package in R was employed to calculate the sensitivity of different drugs. CPXM1 expression was combined with the results of drug sensitivity and a boxplot was drawn. The Wilcoxon signed rank test was used to detect the half inhibitory concentration ($IC_{50}$) between the two subgroups, and statistical significance was set as $p < 0.001$.

### 2.8. R software

The bioinformatics analysis was performed by R software (v4.2.3), and our computer system was Windows 10.

The "limma" package is based on a voom algorithm that enables differential analysis. The "ggplot2," "ggExtra," and "ggpubr" packages are comprehensive and easy-to-understand tools for drawing data graphs. The "survival" package and "survminer" package were designed specifically to process survival data analysis and plot survival curves. The "ComplexHeatmap" and "pheatmap" packages were used to display heat maps. The "circlize" package is an R package specifically designed to draw circles. The "corrplot" package is used to analyze the correlation between the expressions of different genes. The "reshape2" package is an R package for data processing, which is used to implement the exchange of wide format data and long format data.

For gene enrichment analysis, the "org.Hs.eg.db" package is first used for gene ID and symbol conversion. Then, the "clusterProfiler" package is used for functional enrichment and visualization of Gene Ontology (GO) and Kyoto Encyclopedia of Genes and Genomes (KEGG) data. The "enrichplot" package was then applied to implement multiple visualization methods to interpret the enrichment results. Finally, "enrichplot" was used for the functional enrichment plot.

For TME and immune cell infiltration, the full name of ESTIMATE is Estimation of Stromal and Immune cells in Malignant Tumors using Expression data. The "estimate" package uses gene expression data to predict the number of mesenchymal cells and immune cells in malignant tumor tissues. The algorithm is based on the enrichment analysis of gene sets in a single sample, generating three scores: stroma score (which records the presence of stroma in the tumor tissue), immune score (which represents the infiltration of immune cells in the tumor tissue), and estimated score (which deduces tumor purity). CIBERSORT is used to calculate the abundance of immune cells to understand the immune infiltration of the sample. For drug sensitivity analysis, the primary purpose of the "pRRophetic" package is to predict the phenotype of clinical samples from gene expression data.

### 2.9. Statistical analysis

Data were presented via mean ± standard deviation. We performed data analysis via GraphPad Prism 8.0 software (GraphPad Software Inc., La Jolla, CA, USA). Student's t-test and multiple comparison correction were adopted for comparing experimental groups and control groups. And when displaying survival curves, ROC curves are utilized. The association between different genes, as well as association between CPXM1 and percentages of tumor immune cells are depicted by the Pearson coefficient. $P < 0.05$ and $q < 0.2$ were considered statistically significant.

## 3. Results

### 3.1. Over-expression of CPXM1 in GC correlated with poor prognosis

CPXM1 expression data in tumor and adjacent-tumor tissues from different kinds of tumors were downloaded from the TIMER database (http://timer.comp-genomics.org), and the results indicated that CPXM1 expression was elevated in many tumors, including GC (Fig. 1A). Compared with adjacent-tumor tissues, the TCGA data showed that CPXM1 was raised in GC (Fig. 1B). To verify our results, the expression profile data from GSE27342 containing 80 tumor tissues and 80 paired adjacent-tumor tissues were downloaded

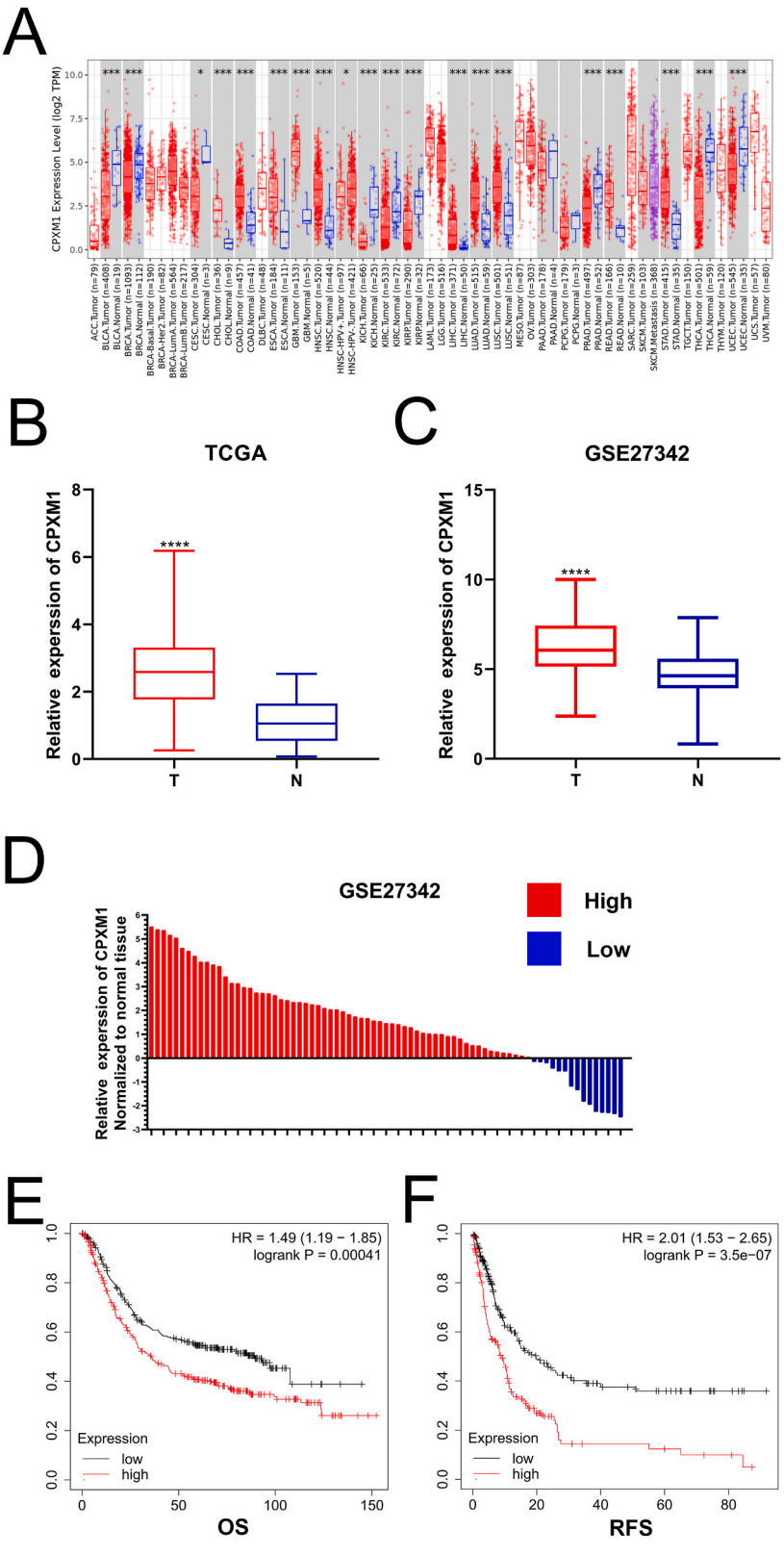


*(caption on next page)*

**Fig. 1. Over-expression of CPXM1 promotes GC and is related to poor prognosis. (A)** Data from TCGA were analyzed for CPXM1 expression between tumor and adjacent-tumor tissues in different kinds of tumors. **(B)** Data on CPXM1 expression levels in GC and adjacent-tumor tissues from TCGA dataset. **(C–D)** Data on CPXM1 expression in GC and adjacent-tumor tissues from the GSE27342 dataset. **(E–F)** Survival analysis of CPXM1 in GC patients.
TCGA, The Cancer Genome Atlas; GC, gastric cancer; ****p < 0.0001.

and the result was consistent with TCGA (Fig. 1C); the expression of CPXM1 was upregulated in more than 80 % of GC tissues (Fig. 1D). Furthermore, Kaplan–Meier survival curves indicated that a high CPXM1 expression level correlated to a poor overall survival and recurrence-free survival (Fig. 1E and F). Over all, CPXM1 is elevated in GC and is associated with a poor prognosis.

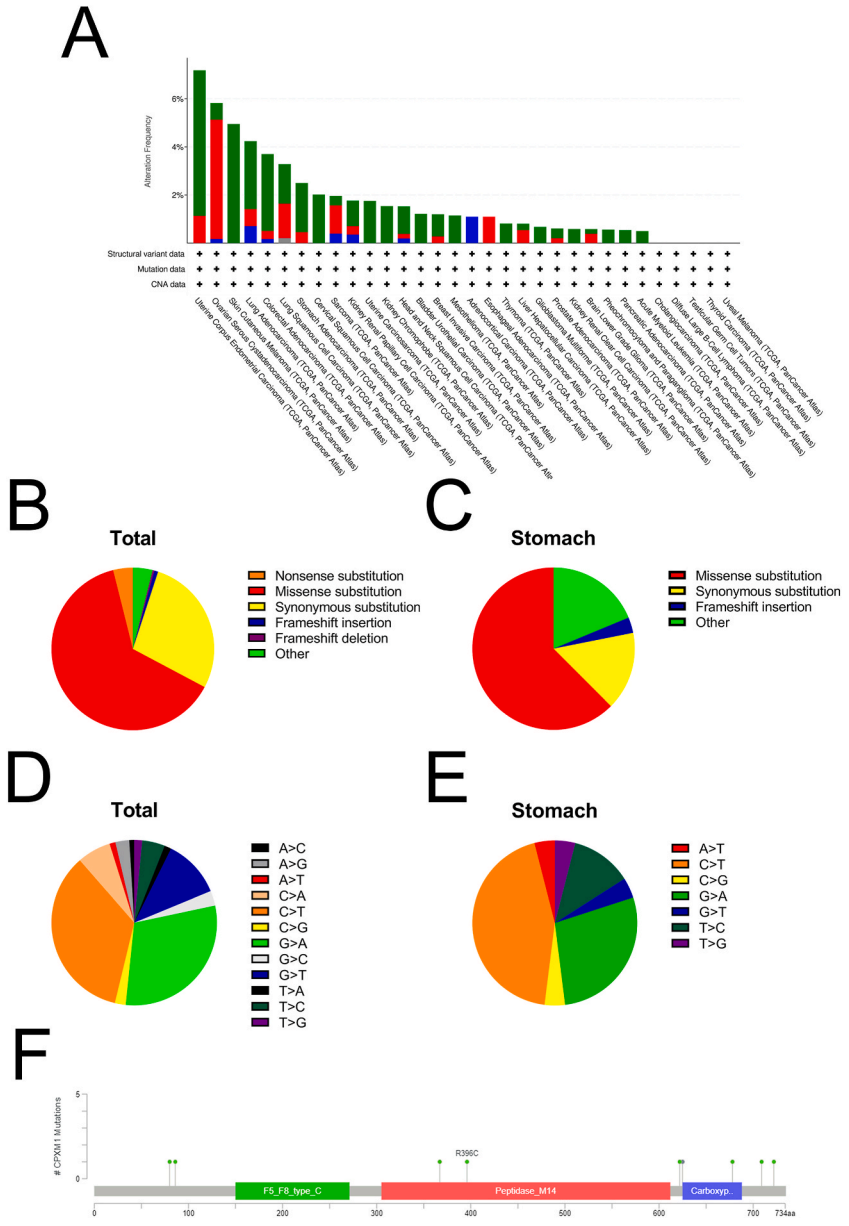


**Fig. 2. Mutations and alternations of CPXM1 in human cancers. (A)** CPXM1 mutation level in TCGA database. **(B–C)** Pie chart conveying mutations of CPXM1 in total tumors and GC. **(D–E)** Pie chart conveying base mutations of CPXM1 in total tumors and GC. **(F)** Mutation points of CPXM1 among amino acids.
TCGA, The Cancer Genome Atlas; GC, gastric cancer.

### 3.2. Mutation and alternation of CPXM1 in human cancers

To explore mutations of CPXM1, data from the COSMIC and cBioPortal databases were utilized. Results showed that the mutation rate is higher in uterine corpus endometrial carcinoma and ovarian serous cystadenocarcinoma (Fig. 2A). The most common mutation of CPXM1 among tumors is a missense mutation (Fig. 2B), which is also the most common in GC (Fig. 2C). Moreover, C > T is the most common mutation in the CPXM1 coding chain in all tumor samples, including GC (Fig. 2D and E). Finally, we examined the common mutation sites of CPXM1, and results indicated the presence of nine mutation sites in CPXM1 between amino acids 0 and 734 (Fig. 2F).

### 3.3. CPXM1 expression and the relationship with clinicopathological factors in GC

The expression of CPXM1 was associated with the following clinicopathological factors: gender (Fig. 3A), grade (Fig. 3B), stage (Fig. 3E) and T (Fig. 3F). But there was no significant difference in age (Fig. 3C), N (Fig. 3D) and M (Fig. 3G). In all, CPXM1 is closely affiliated to gender and different kinds of tumor phases (Fig. 3H).

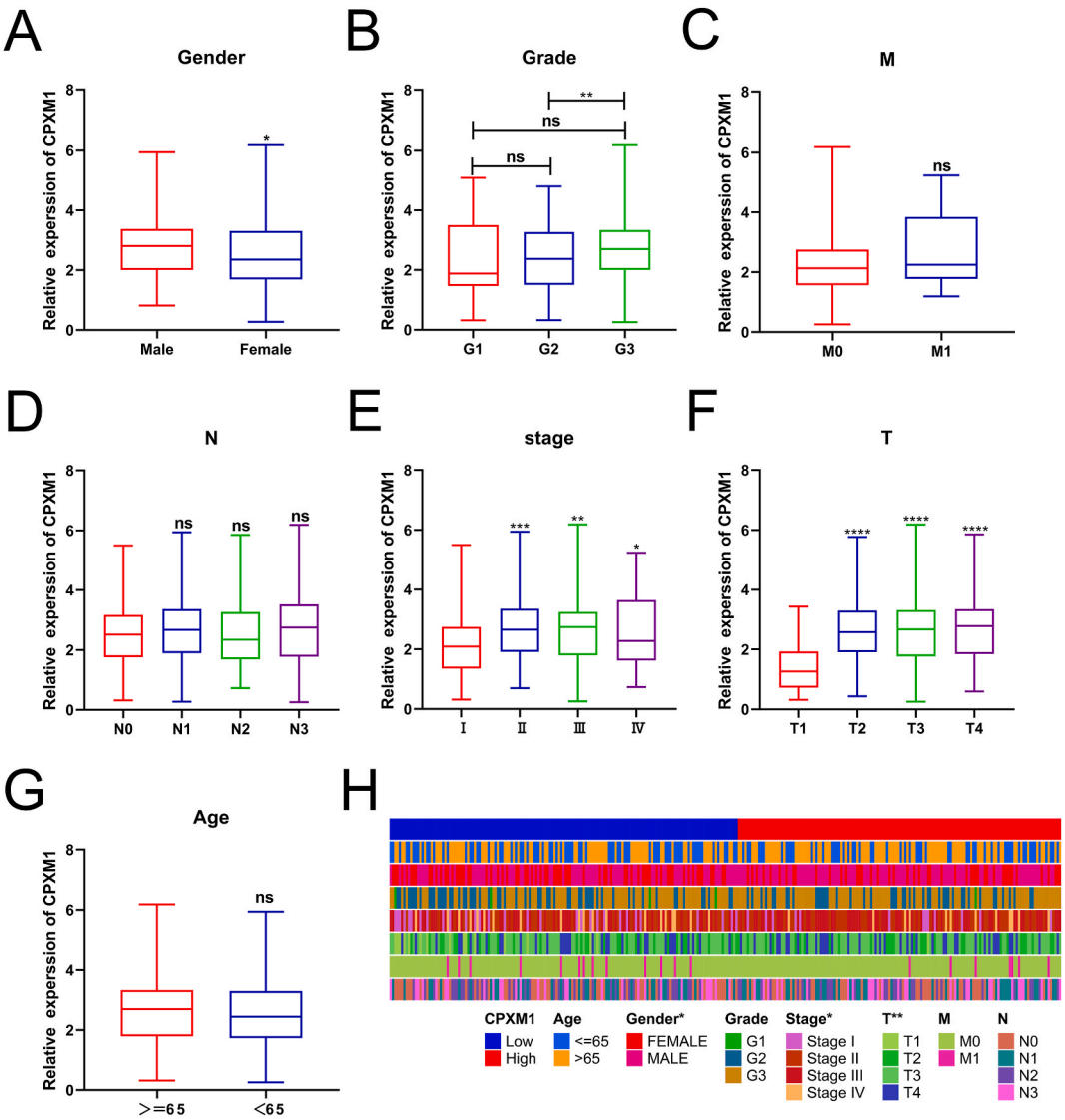


**Fig. 3. CPXM1 expression and its relationship with clinicopathological factors in GC. (A)** Gender, **(B)** histological grade, **(C)** M, **(D)** N, **(E)** T **(F)**, and age **(G)** in GC patients from TCGA. **(H)** Clinicopathological factors presented in a relevant heat map.
TCGA, The Cancer Genome Atlas; GC, gastric cancer. ns $p > 0.05$; *$p < 0.05$; **$p < 0.01$; ***$p < 0.001$; ****$p < 0.0001$.

### 3.4. Identification of potential pathways and downstream targets

Correlation analysis was performed based on profile data of TCGA. In total, 3284 genes were investigated for the mechanism research (Fig. 4A). We analyzed and screened out DEGs. Our study included 667 genes, among which 391 genes were elevated in the high expression group, and 276 genes were downregulated (Fig. 4B). Subsequently, to determine the enriched pathways of the DEGs, GO (Fig. 4C) and KEGG (Fig. 4D) pathway analysis was performed. The results revealed that the PI3K–AKT pathway and TGF-β pathway may be the most important pathways associated with CPXM1.

Next, the STRING website (https://cn.string-db.org/) was used to identify potential proteins that may interact with CPXM1 directly (Fig. 4E). The results showed that DOCK1, FAM196A, PPP2R2B, KLHDC4, FAM129A, ZBTB41, GDAP1, TMEM176B, and c10rf27 are potential downstream targets of CPXM1.

### 3.5. CPXM1 is closely affiliated to the TME and immune cell infiltration

In our study, R software was used to generate the TME score, the stromal score, and the immune score of each GC sample. We found that there was a significant difference between the CPXM1 high and low expression groups. Moreover, the score of the high expression group was significantly higher, indicating that the proportion of stromal cells and immune cells increases with CPXM1 expression

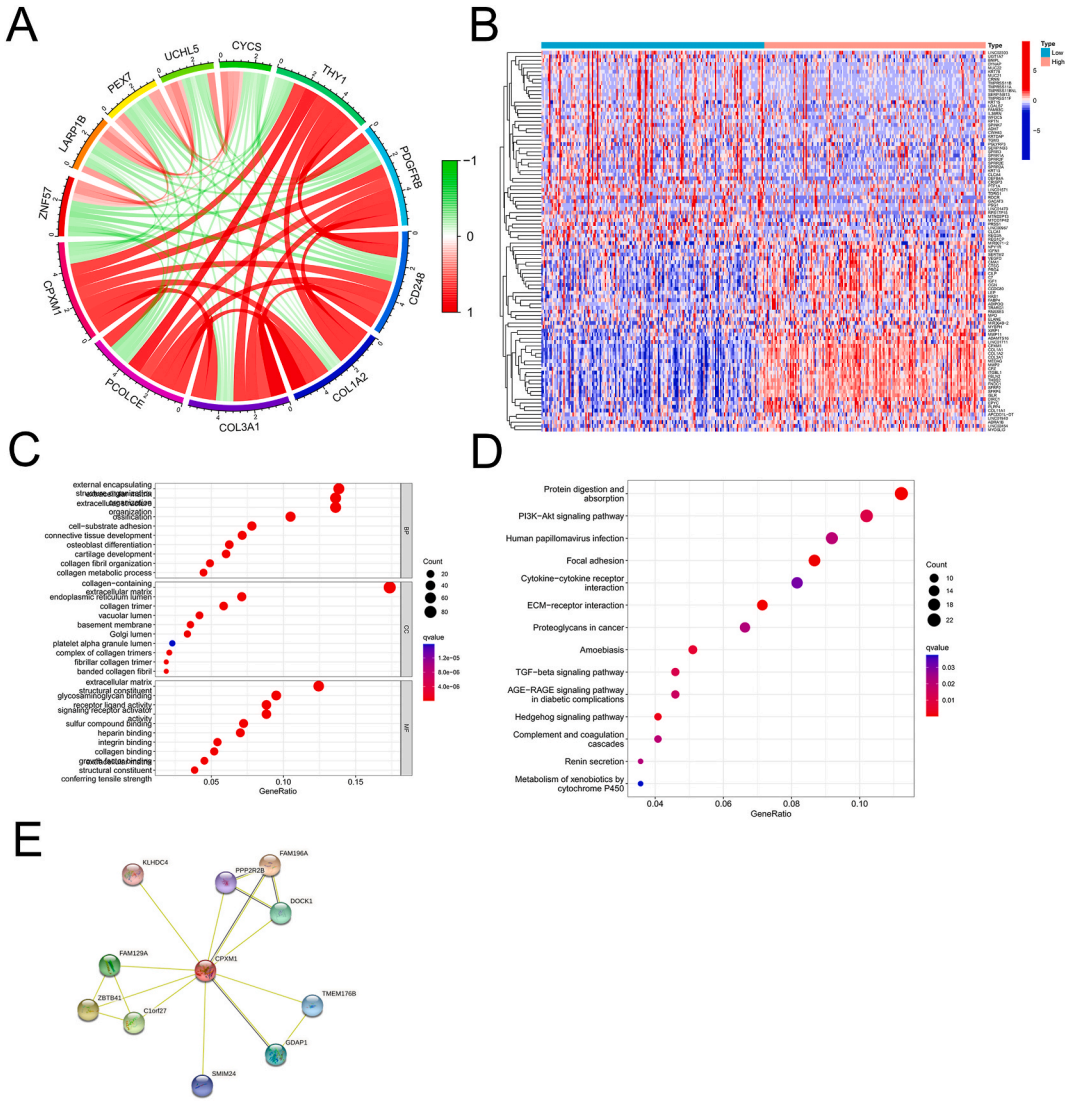


**Fig. 4. Identification of potential pathways and downstream targets.** **(A)** Circle diagram of genes strongly correlated to CPXM1. **(B)** Heat map of differential genes. **(C)** GO analysis of differential genes. **(D)** KEGG analysis of differential genes. **(E)** Proteins that may interact with CPXM1. GO, Gene Ontology; KEGG, Kyoto Encyclopedia of Genes and Genomes; ****$p < 0.0001$.

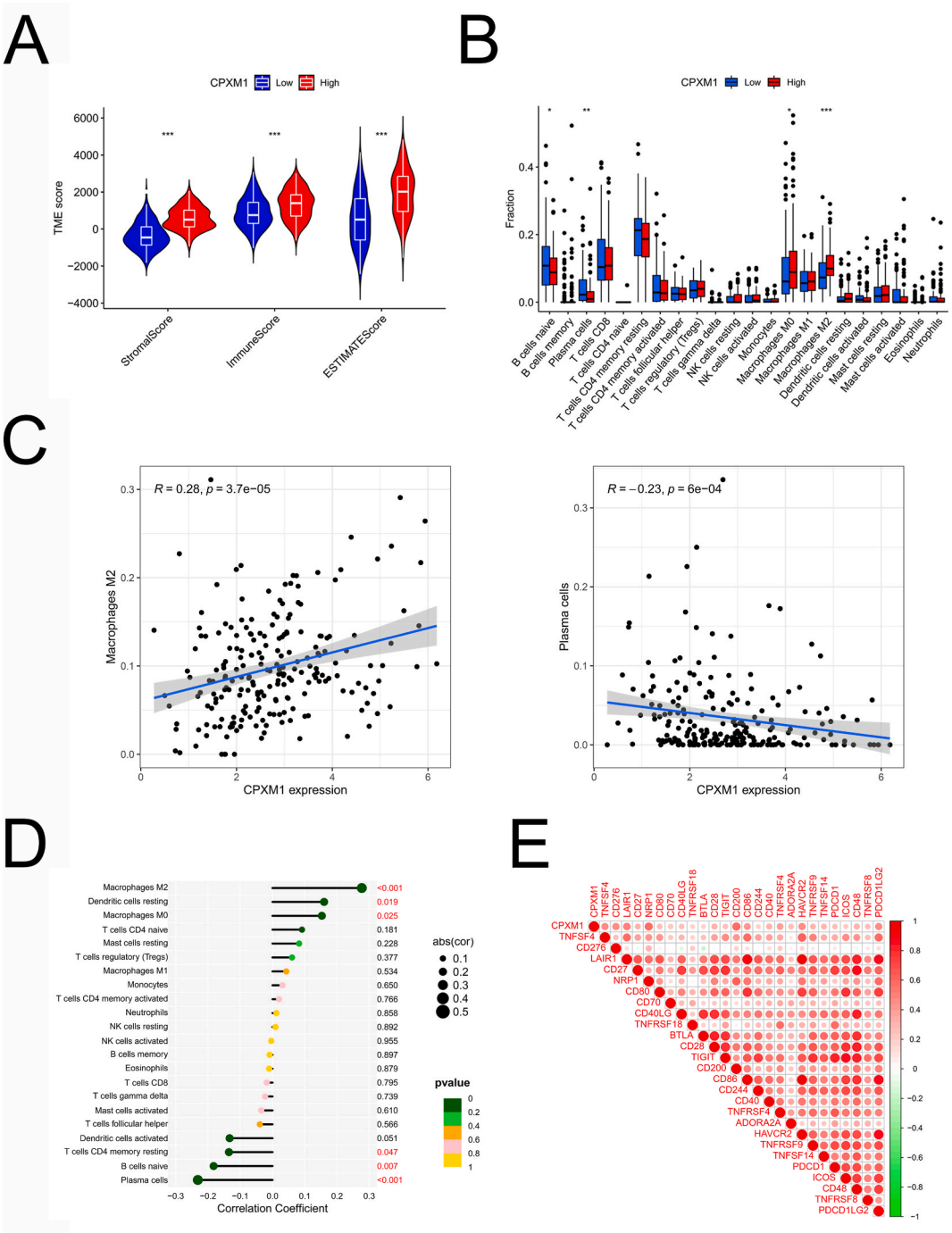


**Fig. 5. CPXM1 is closely related to the TME and immune cell infiltration. (A)** Analysis of differences in the TME. **(B)** Analysis of differences in immune cells. **(C)** Scatter plot of relevant immune cells. **(D)** Correlation analysis of immune cells. **(E)** Correlation analysis of immune checkpoints. TME, tumor microenvironment; *p < 0.05, **p < 0.01, ***p < 0.001.

(Fig. 5A).

Immune cells are important parts of TME. To study the relationship between CPXM1 and immune cells, the proportion of immune cells was calculated and analyzed together with the expression of CPXM1. We found significant differences in the percentage of M2 macrophages and plasma cells in the CPXM1 high and low expression groups (Fig. 5B). In addition, M2 macrophages were proportional to the expression of CPXM1, while the number of plasma cells was inversely related to the expression of CPXM1 (Fig. 5C). Correlation studies also confirmed our results (Fig. 5E). Finally, the correlation analysis determined the immune checkpoints that might be

positively correlated to CPXM1 (Fig. 5F). To sum up, CPXM1 is involved in immune infiltration in the TME.

### 3.6. Drug sensitivity analysis of CPXM1

First, we compared the correlation between the $IC_{50}$ and CPXM1 of various drugs in TCGA GC samples. We screened six drugs that presented significant differences in the $IC_{50}$ among the two groups. It was observed that the $IC_{50}$ of AMG-760 (Fig. 6A), BEZ235 (Fig. 6B), Dasatinib (Fig. 6C), and HG-6-64-1 (Fig. 6E) were downregulated, while the $IC_{50}$ of FH535 (Fig. 6D) and NSC-207895 (Fig. 6F) were upregulated in the CPXM1 high expression group.

## 4. Discussion

CPs play an important physiological role in animal and plant tissues and organs. They are comprised of eight α-helical regions and eight β-structure chains, as well as approximately 45 turns. In summary, α-helices, β-folds, and turns account for at least 90 % of residues [19]. CPs can be divided into three types based on different activity domain centers: SCPs, MCPs, and CCPs.

It is believed that CPs act as a regulator in many human diseases. For example, overexpression of CPE can decrease cell proliferation and increase cell apoptosis [19]. Another study suggested that knocking down of CPE in the liver can alleviate the secretion of serum cholecystokinin, thus promoting the formation of gallstones [20]. Studies have also shown that the elevation of serum pro-CPA and CPA levels can raise the accuracy of diagnosis in pancreatitis [21].

Members of the CP family can often be seen in different kinds of cancers. For example, N-terminal truncated carboxypeptidase E (CPE△N) protein is a mutant form of CPE and is an independent predictor of lung adenocarcinoma (LUAD) recurrence and metastasis. CPE△N can accelerate invasion of LUAD through an E-cadherin-independent pathway [22]. In pancreatic cancer, CPE can regulate cell growth and invasion [23]. Moreover, CPM has the potential to be a therapeutic target [24].

Human physiological and biochemical systems, including malignancies, are significantly influenced by CPXM1. Whole exon sequencing revealed higher expression of CPXM1 in patients with pulmonary benign metastasizing leiomyoma (PBML), indicating that CPXM1 may be employed as a diagnostic and prognostic marker for PBML(34). CPXM1 can affect the TME and the prognosis of immunotherapy in head and neck squamous cell carcinoma (HNSCC) [25]. Polycystic ovary syndrome (PCOS) is a prevalent endocrine condition in women that is accompanied by reproductive and metabolic abnormalities and has an unidentified cause and inadequate therapy. According to several research, CPXM1 concentration in the serum of PCOS mice is up-regulated when compared to normal

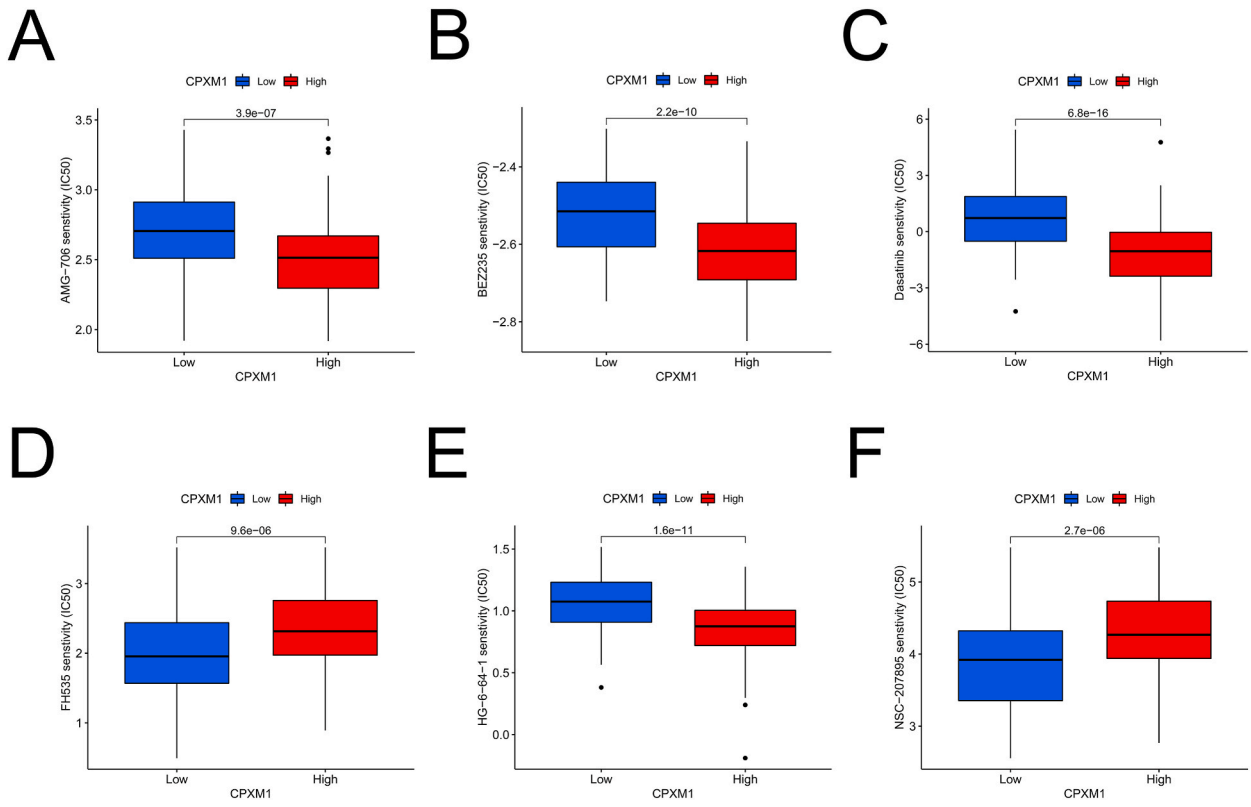


**Figure 6. Drug sensitivity analysis of CPXM1.** Drug sensitivity of **(A)** AMG-706, **(B)** BEZ235, **(C)** Dasatinib, **(D)** FH535, **(E)** HG-6-64-1, and **(F)** NSC-207895.

mice, and it is positively connected with rising serum levels of testosterone and insulin. The levels of CPXM1's mRNA and protein were considerably elevated in the ovarian tissue of PCOS mice. These findings suggest that CPXM1 may be a potential therapeutic target for the treatment of polycystic ovary syndrome [26]. As a new immunotherapeutic target for melanoma, it has been demonstrated that CPXM1 can be utilized as a biomarker to predict the outcome of anti-PD-1 therapy [27].

According to our research, GC patients had higher levels of CPXM1 expression, which is linked to a bad prognosis. Gender, tumor stage, and T stage are all strongly correlated with CPXM1 expression. Furthermore, the PI3K-AKT and TGF- axis may be used by CPXM1 to control the development of GC.

The PI3K–AKT pathway is a classical axis that plays a vital part in various physiological and biochemical activities of normal cells and pathological disorders, cancer included [28]. For instance, CD73 has been shown to promote progression and metastasis of HCC by inducing RAP1-mediated membrane localization of P110β via the PI3K–AKT signaling pathway [29]. Moreover, miR-30D inhibits tumor proliferation and invasion through the SOX4–PI3K–AKT axis in pancreatic cancer, which can predict poor prognosis [30]. Similarly, plasma vesicle-associated proteins promote angiogenesis of cholangiocarcinoma through the DKK1–CKAP4–PI3K axis in cholangiocarcinoma [31].

The TGF-β family includes many kinds of growth factors. Each member can regulate at least one kind of function, including cell proliferation, lineage determination, differentiation, and so on. TGF-β and its downstream markers take on important tasks in almost all biological tissues [32]. For example, knocking down YAP in smooth muscle cells can weaken arterial stiffness and the function of the TGF-β–Smad2/3 signaling pathways in the arteries [33].

TGF-β also acts a big part in human tumors [34]. For instance, EZH2 promotes bone metastasis of breast cancer via the TGF-β signal through the integrin β1-FAK [35]. Similarly, the TGF-β signaling pathway has a positive feedback loop mediated by lncUTGF, and the abnormal regulation of TGF-β can promote HCC metastasis [36].

However, our work has some limitations. First, Transwell and wound-healing experiments are required to further confirm that CPXM1 is involved in the migration and invasion of GC, given that the CPXM1 expression level is correlated with tumor stage and T stage. Second, western blotting is necessary to determine how CPXM1 is connected to the PI3K–AKT and TGF-β pathways. Third, single-cell sequence data are required for additional confirmation because CPXM1 is involved in the TME and immune infiltration.

## 5. Conclusion

Our study suggested that CPXM1 is elevated in GC and is associated with a poor prognosis. The expression of CPXM1 is closely related to gender, tumor stage, and T stage. Moreover, CPXM1 may regulate the progression of GC via the PI3K–AKT and TGF-β axis. Our results also revealed that CPXM1 expression is related to the TME, immune cell infiltration, and drug sensitivity. These findings indicate that deeper research into CPXM1 is necessary because it is anticipated to be a target for the detection and treatment of GC.

Our study does still have some flaws, though. First, there aren't enough samples from our hospital which can back up the TCGA findings; second, there is a lack of experimental proof that CPXM1 controls the PI3K-AKT and TGF-B pathway; and third, there is a lack of proof that CPXM1 can regulate the immune system.

## Author contributions

JZ initiated the study, and QG designed the technology roadmap. QG and LM performed most of the bioinformatics analysis. CL, GX, and NL downloaded RNA-seq and clinicopathological data from TCGA and GEO databases. TZ, GW, and CL performed TME, immune cell infiltration, and drug sensitivity analyses online, respectively. LX and XG drew the figures and edited the manuscript. All of the authors have read and approved the submitted version.

## Funding

The present study was financed by National Natural Science Foundation (Grant Number 81874058 to JZ).

## Data availability statement

The datasets used and/or analyzed during the current study will be made available from the corresponding author on reasonable request.

## Declaration of competing interest

The authors declare that they have no known competing financial interests or personal relationships that could have appeared to influence the work reported in this paper.

## Acknowledgements

The authors would like to thank the Laboratory of Secondary Affiliated Hospital of Nanjing Medical University for providing financial support and technical guidance.

## Appendix A. Supplementary data

Supplementary data to this article can be found online at https://doi.org/10.1016/j.heliyon.2023.e21909.

## References


[1] H. Wu, M. Fu, J. Liu, et al., The role and application of small extracellular vesicles in gastric cancer, Mol. Cancer 20 (2021) 1–19.
[2] R.L. Siegel, K.D. Miller, H.E. Fuchs, A. Jemal, Cancer statistics, 2022. CA, A Cancer Journal for Clinicians 72 (2022) 7–33.
[3] E.C. Smyth, M. Nilsson, H.I. Grabsch, N.C. van Grieken, F. Lordick, Gastric cancer, Lancet 396 (2020) 635–648.
[4] S.S. Joshi, B.D. Badgwell, Current treatment and recent progress in gastric cancer, CA A Cancer J. Clin. 71 (2021) 264–279.
[5] L. Yuan, Z.Y. Xu, S.M. Ruan, S. Mo, J.J. Qin, X.D. Cheng, Long non-coding RNAs towards precision medicine in gastric cancer: early diagnosis, treatment, and drug resistance, Mol. Cancer 19 (2020) 1–22.
[6] H.M. Vedeld, A. Goel, G.E. Lind, Epigenetic biomarkers in gastrointestinal cancers: the current state and clinical perspectives, Semin. Cancer Biol. 51 (2018) 36–49.
[7] M.R. Sapio, L.D. Fricker, Carboxypeptidases in disease: insights from peptidomic studies, Proteonomics Clin. Appl. 8 (2014) 327–337.
[8] D. Atiakshin, A. Kostin, I. Trotsenko, V. Samoilova, I. Buchwalow, M. Tiemann, Carboxypeptidase A3 — A Key Component of the Protease, 2022, pp. 1–23.
[9] C. Liang, D. Carrel, N.K. Singh, L.L. Hiester, I. Fanget, H. Kim, B.L. Firestein, Carboxypeptidase E independently changes microtubule glutamylation, dendritic branching, and neuronal migration, ASN Neuro 14 (2022) 1–15.
[10] V.K. Sharma, X. Yang, S.K. Kim, et al., Novel interaction between neurotrophic factor-α1/carboxypeptidase E and serotonin receptor, 5-HTR1E, protects human neurons against oxidative/neuroexcitotoxic stress via β-arrestin/ERK signaling, Cell. Mol. Life Sci. 79 (2022) 1–19.
[11] Y.H. Kim, H.M. O'Neill, J.P. Whitehead, Carboxypeptidase X-1 (CPX-1) is a secreted collagen-binding glycoprotein, Biochem. Biophys. Res. Commun. 468 (2015) 894–899.
[12] Y.H. Kim, J.L. Barclay, J. He, et al., Identification of carboxypeptidase X (CPX)-1 as a positive regulator of adipogenesis, FASEB (Fed. Am. Soc. Exp. Biol.) J. 30 (2016) 2528–2540.
[13] M. Zheng, J. Long, A. Chelariu-Raicu, et al., Identification of a novel tumor microenvironment prognostic signature for advanced-stage serous ovarian cancer, Cancers 13 (2021).
[14] Mao X. hong, Q. Ye, G bing Zhang, et al., Identification of differentially methylated genes as diagnostic and prognostic biomarkers of breast cancer, World J. Surg. Oncol. 19 (2021) 1–11.
[15] Y. Chen, Z.Y. Li, G.Q. Zhou, Y. Sun, An immune-related gene prognostic index for head and neck squamous cell carcinoma, Clin. Cancer Res. 27 (2021) 330–341.
[16] Y.H. Wang, C.C. Lin, C.Y. Yao, et al., A 4-gene leukemic stem cell score can independently predict the prognosis of myelodysplastic syndrome patients, Blood Advances 4 (2020) 644–654.
[17] A. Kumar, O.R. Bandapalli, N. Paramasivam, et al., Familial Cancer Variant Prioritization Pipeline version 2 (FCVPPv2) applied to a papillary thyroid cancer family, Sci. Rep. 8 (2018) 1–12.
[18] Z. Liu, L.L. Hong, Zheng J. Sen, et al., Comprehensive transcriptomic profiling and mutational landscape of primary gastric linitis plastica, Gastric Cancer 26 (2023) 203–219.
[19] J. Li, Z. Dong, Y. Pan, L. Wang, W. Zhao, J. Zhang, CPE Regulates Proliferation and Apoptosis of Primary Myocardial Cells Mediated by Ischemia and Hypoxia Injury, 2022, p. 2022.
[20] S.L. Dai, J. Zhou, K.X. Yang, S.Y. Yang, The expression of hepatic carboxypeptidase e is decreased in patients with cholesterol gallstone, Saudi J. Gastroenterol. 21 (2015) 226–231.
[21] O. Kemik, A.S. Kemik, A. Sumer, H. Beğenik, A.C. Dülger, S. Purisa, S. Tuzun, Serum procarboxypeptidase A and carboxypeptidase A levels in pancreatic disease, Hum. Exp. Toxicol. 31 (2012) 447–451.
[22] J. Sun, D. Meng, T. Yu, et al., N-terminal truncated carboxypeptidase E represses E-cadherin expression in lung cancer by stabilizing the Snail-HDAC complex, Am. J. Cancer Res. 10 (2020) 925–938.
[23] Z. Bai, M. Feng, Y. Du, L. Cong, Y. Cheng, Carboxypeptidase e down-regulation regulates transcriptional and epigenetic profiles in pancreatic cancer cell line: a network analysis, Cancer Biomarkers 29 (2020) 79–88.
[24] C. Pisano, I. Vlodavsky, N. Ilan, F. Zunino, The potential of heparanase as a therapeutic target in cancer, Biochem. Pharmacol. 89 (2014) 12–19.
[25] S. Chen, Y. Yang, S. He, M. Lian, R. Wang, J. Fang, Review of biomarkers for response to immunotherapy in HNSCC microenvironment, Front. Oncol. 13 (2023) 1–11.
[26] S. Pervaz, A. Ullah, E.A. Adu-Gyamfi, J. Lamptey, S.K. Sah, M.J. Wang, Y.X. Wang, Role of CPXM1 in impaired glucose metabolism and ovarian dysfunction in polycystic ovary syndrome, Reprod. Sci. 30 (2023) 526–543.
[27] L. Tian, F. Long, Y. Hao, et al., A cancer associated fibroblasts-related six-gene panel for anti-PD-1 therapy in melanoma driven by weighted correlation network analysis and supervised machine learning, Front. Med. 9 (2022) 1–18.
[28] D. Tewari, P. Patni, A. Bishayee, A.N. Sah, A. Bishayee, Natural products targeting the PI3K-Akt-mTOR signaling pathway in cancer: a novel therapeutic strategy, Semin. Cancer Biol. 80 (2022) 1–17.
[29] X.L. Ma, M.N. Shen, B. Hu, et al., CD73 promotes hepatocellular carcinoma progression and metastasis via activating PI3K/AKT signaling by inducing Rap1-mediated membrane localization of P110β and predicts poor prognosis, J. Hematol. Oncol. 12 (2019) 1–17.
[30] X. Xu, K. Zong, X. Wang, D. Dou, P. Lv, Z. Zhang, H. Li, miR-30d suppresses proliferation and invasiveness of pancreatic cancer by targeting the SOX4/PI3K-AKT axis and predicts poor outcome, Cell Death Dis. 12 (2021).
[31] Y. Wang, H. Yu, X. Xie, et al., Plasmalemma vesicle-associated protein promotes angiogenesis in cholangiocarcinoma via the DKK1/CKAP4/PI3K signaling pathway, Oncogene 40 (2021) 4324–4337.
[32] C.B. Program, TGF- β SIGNAL TRANSDUCTION, 1998.
[33] H.D.A. Stiffness, Yes-Associated Protein Targets the Transforming, 2022, pp. 851–867.
[34] E. Batlle, J. Massagué, Transforming growth factor-β signaling in immunity and cancer, Immunity 50 (2019) 924–940.
[35] Zhang L, Qu J, Qi Y, et al.: Activation. 1–16..
[36] M.Z. Wu, Y chuan Yuan, B.Y. Huang, J.X. Chen, B.K. Li, J.H. Fang, S.M. Zhuang, Identification of a TGF-β/SMAD/lnc-UTGF positive feedback loop and its role in hepatoma metastasis, Signal Transduct. Targeted Ther. 6 (2021).